532.516:621.822.5

Paper No. 210-23

Influence of Gas Inertia Forces Generated Within the Stabilizing Restrictor on Dynamic Characteristics of Externally Pressurized Thrust Gas Bearings*

(1st Report, Case of Laminar Flow at the Capillary Restriction)

By Yoshio HARUYAMA** and Haruo MORI***

In this paper, the authors investigated theoretically and experimentally the influence of the gas inertia forces generated within the stabilizing restrictor on the dynamic characteristics of externally pressurized circular thrust gas bearings with a stabilizer.

From comparison with the experiment, it may be concluded that the influence on the dynamic characteristics should be considerable, and that the presented analysis yields good predictions for both the bearing stiffness and the damping coefficient in a wide range of designing conditions.

Key Words: Lubrication, Bearing, Externally Pressurized Thrust Bearing, Dynamic Characteristics, Inertia Effect, Capillary Restriction, Laminar Flow

1. Introduction

Conventional analyses of the dynamic performances of externally pressurized gas bearings are based on the equation in which the inertia forces of a gas are ignored. A significant influence of the gas inertia forces on the dynamic characteristics has been reported recently[1]~[3]. In conventional studies of externally pressurized bearings, only the inertia forces generated at the bearing clearance have been considered but one generated at the restricted part is neglected. In the previous report[4], we investigated the influence of the fluid inertia forces generated within the supply capillary restriction on the dynamic characteristics of externally pressurized circular thrust bearings and pointed out that the influence should be considerable when the kinematic viscosity of the lubricant becomes too low.

The present report is concerned with the influence of the gas inertia forces generated within the stabilizing capillary restriction on the dynamic characteristics of externally pressurized thrust gas bearings. The bearings with a stabilizer investigated here are shown in Figs.1 and 2. Mori, et al.[5],[6] have investigated the fundamental characteristics of these bearings. However, it may be necessary to examine the effect of gas inertia forces on the bearings with a large diameter capillary restriction.

2. Nomenclature

a : radius of capillary
b, B : damping coefficient
c_D : discharge coefficient
c_0 : velocity of sound
f : frequency
h, H : bearing clearance
h_r, H_r : depth of recess
h_0 : equilibrium clearance
k , K : stiffness
l : length of capillary
m : mass of shaft
m_1 : mass flow rate through supply restrictor
m_2 : mass flow rate through stabilizing restrictor
m_3 : mass flow rate through bearing gap
n : number of capillaries
p, P : pressure
p_a : ambient pressure
p_c, P_C : fluid capacity pressure
$P_{Cr0} = \frac{P_{C0} + P_{r0}}{2}$
p_r, P_r : recess pressure
p_s, P_S : supply pressure
r, R : radial coordinate
r_c, r_c' : radial coordinate of capillary
r_s : radius of supply orifice
r_0 : outer radius of bearing
r_1, R_1 : radius of recess
$\mathfrak{R}$: gas constant
T : absolute temperature
t : time

* Received 13th November, 1980 ; 8th May, 1981.

** Instructor, Faculty of Engineering, Toyama University, 1-1, Nakagawa-Sonomachi, Takaoka, Japan.

*** Professor, Faculty of Engineering, Kyoto University, Yoshida-Honmachi, Sakyo-ku, Kyoto, Japan.

V_C : volume of fluid capacity
V_r : volume of recess
x : axial coordinate

$\alpha = \frac{\rho_0 a^2 p_a}{12\mu^2}\left(\frac{h_0}{r_0}\right)^2$: inertia parpmeter

$\beta = \frac{p_a l}{12\mu c_0}\left(\frac{h_0}{r_0}\right)^2$: compressibility parameter

$\Gamma = -\frac{12\mu c_D r_s^2\sqrt{\Re T}}{p_a h_0^3}\ln R_1$: feeding parameter

$\gamma = \frac{8\mu c_D r_s^2\sqrt{\Re T}\, l}{n a^4 p_a}$ or $= -\frac{3na^4}{2lh_0^3}\ln R_1$

$\delta = \frac{2lV_c}{3n\pi a^4}\left(\frac{h_0}{r_0}\right)^2$

δ_0 : logarithmic decrement
$\zeta = a^2\omega/\nu_0$

$\eta = \frac{i\omega}{c_0}\left\{1 - \frac{2J_1(\sqrt{-i\zeta})}{\sqrt{-i\zeta}\,J_0(\sqrt{-i\zeta})}\right\}^{-1/2}$

κ : adiabatic index
μ : viscosity
ν_0 : kinematic viscosity
ρ_C : density of gas within fluid capacity
ρ_r : density of gas within recess
ρ_0 : density of gas (constant)

$\sigma = \frac{12\mu\omega}{p_a}\left(\frac{r_0}{h_0}\right)^2$: squeeze number

$\tau = \omega t$: dimensionless time
ω : angular speed of squeeze motion

In the case of two symbols, the former is a dimensional quantity and the latter is a dimensionless quantity.

3. Theoretical analysis

The externally pressurized circular thrust gas bearings with a stabilizer analyzed here are shown schematically in Figs. 1 and 2, in which some symbols used are slso noted.
The stabilizer consists of a fluid capacity and a capillary restriction. Fig. 1 shows a bearing(Type A) of which the stabilizer is inserted into the gas-supply line and Fig.2 shows a bearing(Type B) of which the stabilizer is connected to the bearing recess.
In this analysis, the supply restrictor consists of an orifice whose radius is r_s and the capillary restriction consists of some straight circular pipes whose radius is a and length is l.

3.1 Assumptions

The following assumptions are made in order to simplify the analysis.
(1) The flow through the bearing gap is viscous so that the pressure follows Reynolds equation.
(2) The depth of the recess is large enough compared with the bearing clearance so that the recess pressure may be uniform and it may be equal to the bearing gap pressure at $r = r_1$.
(3) The flow through capillary restriction is laminar and the inlet is so short that it may be neglected.
(4) The change of state of the gas is isothermal.
(5) The thrust plate is paralled to the bearing surface.

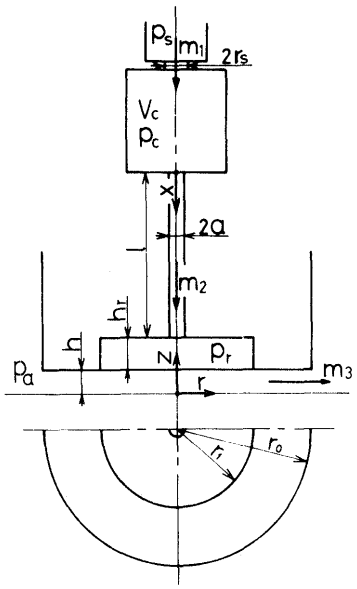

Fig.1 Coordinate system for thrust bearing (Type A)

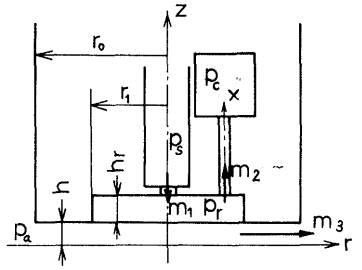

Fig.2 Coordinate system for thrust bearing (Type B)

3.2 Fundamental equations

The dimensionless bearing pressure follows the dimensionless Reynolds equation as follows under the assumptions (1), (4) and (5)

$$\frac{H^3}{R}\frac{\partial}{\partial R}\left[RP\frac{\partial P}{\partial R}\right] = \sigma\frac{\partial(PH)}{\partial\tau} \qquad (1)$$

where

$$P = \frac{p}{p_a},\quad H = \frac{h}{h_0},\quad R = \frac{r}{r_0},\quad \tau = \omega t$$

$$\sigma = \frac{12\mu\omega}{p_a}\left(\frac{r_0}{h_0}\right)^2 \quad : \text{squeeze number}$$

Taking a small sinusoidal vibration which occurs around the equilibrium state of bearing into consideration, the dimensionless clearance, H, may be given by

$$H(\tau) = 1 + \varepsilon\sin\tau \qquad (2)$$

The dimensionless bearing pressure, P , is asumed as

$$P(R,\tau) = P_0(R) + \varepsilon\{P_1(R)\sin\tau + P_2(R)\cos\tau\} \qquad (3)$$

Substituting Eqs. (2) and (3) into Eq. (1), we obtain the following fundamental equations for $P_0 \sim P_2$ [7]

$$\frac{d}{dR}\left[R\frac{dP_0^2}{dR}\right] = 0 \qquad (4)$$

$$\frac{1}{R}\frac{d}{dR}\left[R\frac{d(P_0P_1)}{dR}\right]=-\sigma P_2 \qquad (5)$$

$$\frac{1}{R}\frac{d}{dR}\left[R\frac{d(P_0P_2)}{dR}\right]=\sigma(P_0+P_1) \qquad (6)$$

3.3 Boundary conditions

The boundary conditions for the bearing(Type A) can be written in the forms,

$$P_0|_{R=1}=1,\quad P_1|_{R=1}=P_2|_{R=1}=0 \qquad (7)$$

$$m_2|_{x=0}=m_1-\frac{\partial}{\partial t}(\rho_c V_c) \qquad (8)$$

$$m_3|_{r=r_1}=m_2|_{x=l}-\frac{\partial}{\partial t}(\rho_r V_r) \qquad (9)$$

where m_1, m_2 and m_3 are the mass flow rates through the supply restriction, the stabilizing restrictor and the bearing gap respectively. m_1 and m_3 are given by

$$m_1=\frac{c_D\pi r_s^2 p_a}{\sqrt{\Re T}}P_s\phi \qquad (10)$$

$$m_3=-\frac{\pi h_0^3 p_a^2}{12\mu\Re T}RH^3\frac{\partial P^2}{\partial R} \qquad (11)$$

where

$$\left.\begin{aligned}\phi&=\left(\frac{2\kappa}{\kappa-1}\right)^{1/2}\left(\frac{P_c}{P_s}\right)^{1/\kappa}\left[1-\left(\frac{P_c}{P_s}\right)^{(\kappa-1)/\kappa}\right]^{1/2}\\ &\quad : \frac{P_c}{P_s}>\left(\frac{2}{\kappa+1}\right)^{\kappa/(\kappa-1)}\\ &=\left(\frac{2\kappa}{\kappa+1}\right)^{1/2}\left(\frac{2}{\kappa+1}\right)^{1/(\kappa-1)}\\ &\quad : \frac{P_c}{P_s}\leqq\left(\frac{2}{\kappa+1}\right)^{\kappa/(\kappa-1)}\end{aligned}\right\} \qquad (12)$$

We now consider m_2. For unsteady an viscous compressible laminar flow through a straight circular pipe when the inlet pressure and the outlet pressure $p_{01}+p_{11}e^{i\omega t}$ and $p_{02}+p_{12}e^{i\omega t}$ respectively, the velocity component in axial direction is given by [8]

$$u=\frac{a^2(p_{01}-p_{02})}{4\rho_0\nu_0 l}(1-r_c'^2)-\frac{1}{i\omega\rho_0}\left[\frac{\eta l}{e^{\eta l}-e^{-\eta l}}\frac{p_{12}(e^{\eta x}+e^{-\eta x})+p_{11}\{e^{\eta(l-x)}+e^{-\eta(l-x)}\}}{l}\right]$$
$$\times\left\{1-\frac{J_0(r_c'\sqrt{-i\zeta})}{J_0(\sqrt{-i\zeta})}\right\}e^{i\omega t} \qquad (13)$$

where

$$r_c'=r_c/a,\quad \zeta=\omega a^2/\nu_0,\quad i=\sqrt{-1},\quad \eta=\frac{i\omega}{c_0}\left\{1-\frac{2J_1(\sqrt{-i\zeta})}{\sqrt{-i\zeta}\,J_0(\sqrt{-i\zeta})}\right\}^{-1/2},$$

J_0, J_1 are Bessel functions of the first kind. Assuming the fluid capacity pressure and the recess pressure as

$$P_c=P_{c0}+\varepsilon(P_{c1}\sin\tau+P_{c2}\cos\tau) \qquad (14),\qquad P_r=P_{r0}+\varepsilon(P_{r1}\sin\tau+P_{r2}\cos\tau) \qquad (15)$$

we get the following equations for $m_2|_{x=0}$, $m_2|_{x=l}$

$$m_2|_{x=0}=\frac{n\pi a^4 p_a^2}{8\mu\Re Tl}P_{cr0}\{(P_{c0}-P_{r0})+(D_1P_{c1}+D_2P_{c2}+D_3P_{r1}+D_4P_{r2})\varepsilon\sin\tau$$
$$+(D_1P_{c2}-D_2P_{c1}+D_3P_{r2}-D_4P_{r1})\varepsilon\cos\tau\} \qquad (16)$$

$$m_2|_{x=l}=\frac{n\pi a^4 p_a^2}{8\mu\Re Tl}P_{cr0}\{(P_{c0}-P_{r0})-(D_1P_{r1}+D_2P_{r2}+D_3P_{c1}+D_4P_{c2})\varepsilon\sin\tau$$
$$-(D_1P_{r2}-D_2P_{r1}+D_3P_{c2}-D_4P_{c1})\varepsilon\cos\tau\} \qquad (17)$$

where

$$\rho_0=p_aP_{cr0}/(\Re T),\quad P_{cr0}=(P_{c0}+P_{r0})/2$$

$$D_1=A_1\xi_2+A_2\xi_1,\quad D_2=A_1\xi_1-A_2\xi_2,\quad D_3=-A_3\xi_2-A_4\xi_1,\quad D_4=-A_3\xi_1+A_4\xi_2$$

ξ_1, ξ_2 and $A_1\sim A_4$ are real variables which are defined by

$$\frac{J_1(\sqrt{-i\zeta})}{J_0(\sqrt{-i\zeta})}\equiv\frac{\sqrt{-i\zeta}}{2}-\frac{\zeta\sqrt{-i\zeta}}{16}(\xi_1+i\xi_2) \qquad (18)$$

$$\eta l(e^{\eta l}+e^{-\eta l})/(e^{\eta l}-e^{-\eta l})\equiv A_1+iA_2 \qquad (19),\qquad 2\eta l/(e^{\eta l}-e^{-\eta l})\equiv A_3+iA_4 \qquad (20)$$

ζ and η are dimensionless parameters which represent the gas inertia forces and the gas compressibility. Now we put

$$\zeta\equiv\alpha\sigma \qquad (21),\qquad \eta l\equiv\frac{i\beta\sigma}{1-[\{2J_1(\sqrt{-i\zeta})\}/\{\sqrt{-i\zeta}\,J_0(\sqrt{-i\zeta})\}]} \qquad (22)$$

where α and β are dimensionless parameters which, respectively, can be expressed by

$$\alpha=\frac{\rho_0a^2p_a}{12\mu^2}\left(\frac{h_0}{r_0}\right)^2 \qquad (23),\qquad \beta=\frac{p_al}{12\mu c_0}\left(\frac{h_0}{r_0}\right)^2 \qquad (24)$$

α and β are new parameters which have never appeared in the conventional analysis. These parameters may be named the inertia parameter and the compressibility parameter respectively in this paper.

m_2 is given by treating quasisteadily the flow rate through the capillary as follows[6]

$$m_2=\frac{n\pi a^4 {p_a}^2}{16\mu\Re Tl}({P_c}^2-{P_r}^2)\fallingdotseq\frac{n\pi a^4 {p_a}^2}{8\mu\Re Tl}\Big[P_{cr0}\{(P_{c0}-P_{r0})+(P_{c1}-P_{r1})\varepsilon\sin\tau$$
$$+(P_{c2}-P_{r2})\varepsilon\cos\tau\}+\frac{P_{c0}-P_{r0}}{2}\{(P_{c1}+P_{r1})\varepsilon\sin\tau+(P_{c2}+P_{r2})\varepsilon\cos\tau\}\Big] \tag{25}$$

Substituting Eqs. (10), (11), (2) and (14) ~ (17) into Eqs. (8) and (9), we obtain the following equations as boundary conditions for the bearing(Type A)

$$\left.\frac{dP_0^2}{dR}\right|_{R=R_1}=-\frac{\Gamma P_s\phi_0}{\phi} \tag{26}$$
$$\gamma P_s\phi_0=P_{cr0}(P_{c0}-P_{r0}) \tag{27}$$
$$\left.\frac{d(P_0P_1)}{dR}\right|_{R=R_1}=\frac{\Gamma}{\phi\gamma}P_{cr0}\Big\{\frac{3}{2}(P_{c0}-P_{r0})+\frac{1}{2}(D_1P_{r1}$$
$$+D_2P_{r2}+D_3P_{c1}+D_4P_{c2})\Big\}-\frac{1}{2}\sigma R_1(1+H_r)\left.\frac{P_0P_2}{P_{r0}}\right|_{R=R_1} \tag{28}$$
$$\left.\frac{d(P_0P_2)}{dR}\right|_{R=R_1}=\frac{\Gamma}{2\phi\gamma}P_{cr0}(D_1P_{r2}-D_2P_{r1}+D_3P_{c2}-D_4P_{c1})+\frac{1}{2}\sigma R_1\Big\{P_{r0}+(1+H_r)\left.\frac{P_0P_1}{P_{r0}}\right|_{R=R_1}\Big\} \tag{29}$$
$$P_{cr0}(D_1P_{c1}+D_2P_{c2}+D_3P_{r1}+D_4P_{r2})=-2\gamma P_s\phi_0AP_{c1}+\delta\sigma P_{c2} \tag{30}$$
$$P_{cr0}(D_1P_{c2}-D_2P_{c1}+D_3P_{r2}-D_4P_{r1})=-2\gamma P_s\phi_0AP_{c2}-\delta\sigma P_{c1} \tag{31}$$

where

$$\phi=\phi_0-2\phi_0A\varepsilon(P_{c1}\sin\tau+P_{c2}\cos\tau)\quad,\qquad\phi_0=\phi|_{P_c=P_{c0}}\quad,\qquad A=-\frac{1}{2\phi_0}\left.\frac{\partial\phi}{\partial P_c}\right|_{P_c=P_{c0}}$$
$$\Gamma=-\frac{12\mu c_D r_s^2\sqrt{\Re T}}{p_a h_0^3}\ln R_1\quad,\qquad\gamma=\frac{8\mu c_D r_s^2\sqrt{\Re T}l}{na^4p_a}\quad,\qquad\delta=\frac{2lV_c}{3n\pi a^4}\left(\frac{h_0}{r_0}\right)^2$$
$$\phi=-R_1\ln R_1$$

In the same manner as the above, the boundary conditions for the bearing(Type B) can be obtained in the forms,

$$\left.\frac{dP_0^2}{dR}\right|_{R=R_1}=-\frac{\Gamma P_s\phi_0}{\phi} \tag{32}$$
$$\left.\frac{d(P_0P_1)}{dR}\right|_{R=R_1}=\frac{\Gamma P_s\phi_0}{\phi}\Big[\frac{3}{2}+\frac{A}{P_{r0}}(P_0P_1)\Big]_{R=R_1}-\frac{\sigma}{2}R_1(1+H_r)\left.\frac{P_0P_2}{P_{r0}}\right|_{R=R_1}$$
$$+\frac{\gamma P_{r0}}{2\phi}(D_1P_{r1}+D_2P_{r2}+D_3P_{c1}+D_4P_{c2}) \tag{33}$$
$$\left.\frac{d(P_0P_2)}{dR}\right|_{R=R_1}=\frac{\Gamma P_s\phi_0}{\phi}\Big[\frac{A}{P_{r0}}(P_0P_2)\Big]_{R=R_1}+\frac{\sigma}{2}R_1\Big[P_{r0}+(1+H_r)\frac{P_0P_1}{P_{r0}}\Big]_{R=R_1}$$
$$+\frac{\gamma P_{r0}}{2\phi}(D_1P_{r2}-D_2P_{r1}+D_3P_{c2}-D_4P_{c1}) \tag{34}$$
$$P_{r0}(D_1P_{c1}+D_2P_{c2}+D_3P_{r1}+D_4P_{r2})=\delta\sigma P_{c2} \tag{35}$$
$$P_{r0}(D_1P_{c2}-D_2P_{c1}+D_3P_{r2}-D_4P_{r1})=-\delta\sigma P_{c1} \tag{36}$$

where

$$\phi_0=\phi|_{Pr=Pr0},\qquad A=-\frac{1}{2\phi_0}\left.\frac{\partial\phi}{\partial P_r}\right|_{Pr=Pr0}$$
$$\gamma=-\frac{3na^4}{2lh_0^3}\ln R_1$$
$$\phi=\left(\frac{2\kappa}{\kappa-1}\right)^{1/2}\left(\frac{P_r}{P_s}\right)^{1/\kappa}\left[1-\left(\frac{P_r}{P_s}\right)^{(\kappa-1)/\kappa}\right]^{1/2}:$$
$$\frac{P_r}{P_s}\geqq\left(\frac{2}{\kappa+1}\right)^{\kappa/(\kappa-1)}$$
$$=\left(\frac{2\kappa}{\kappa+1}\right)^{1/2}\left(\frac{2}{\kappa+1}\right)^{1/(\kappa-1)}:$$
$$\frac{P_r}{P_s}\leqq\left(\frac{2}{\kappa+1}\right)^{\kappa/(\kappa-1)}$$

3.4 Dimensionless stiffness and dimensionless damping coefficient

P_0 ~ P_2 can be analyzed by solving the fundamental equations, Eqs. (4) ~ (6) under the boundary conditions. P_0 is given by[7]

$$P_0^2=\frac{P_{r0}^2-1}{\ln R_1}\ln R+1 \tag{37}$$

P_1 and P_2 are obtained by Runge-Kutta-Gill method, because these are insoluble analytically.

The dimensionless stiffness, K , and the dimensionless damping coefficient, B , respectively, are defined by

$$K=\frac{h_0}{\pi {r_0}^2 p_a}k$$

$$=-2\int_0^{R_1} P_{r1}RdR-2\int_{R_1}^{1} P_1RdR \qquad (38)$$

$$B=\frac{h_0\,\omega}{\pi r_0^2 p_a}b$$

$$=-2\int_0^{R_1} P_{r2}RdR-2\int_{R_1}^{1} P_2RdR \qquad (39)$$

Finally, both K and B can be derived using the seven conventional dimensionless designing parameters: Γ, P_s, R_1, H_f, γ, δ, σ and two new dimensionless parameters: α (the inertia parameter) and β (the compressibility parameter). The influence of the gas inertia forces within the capillary restriction on the dynamic characteristics can be determined by α and β.

4. Examples of calculated results

Examples of calculated results for R_1=0.5, H_f=10, γ=0.5 (Type A), 10 (Type B) and δ=100 are given in Figs.3 to 10. In these figures, the theoretical results

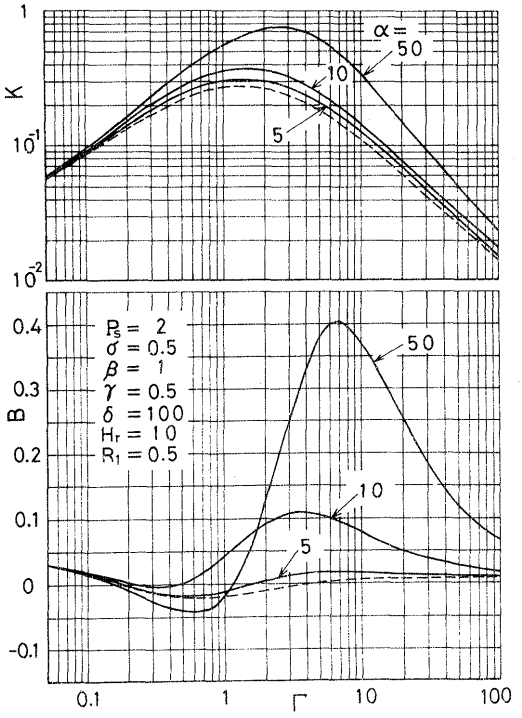

Fig.3 K, B for different α (Type A)

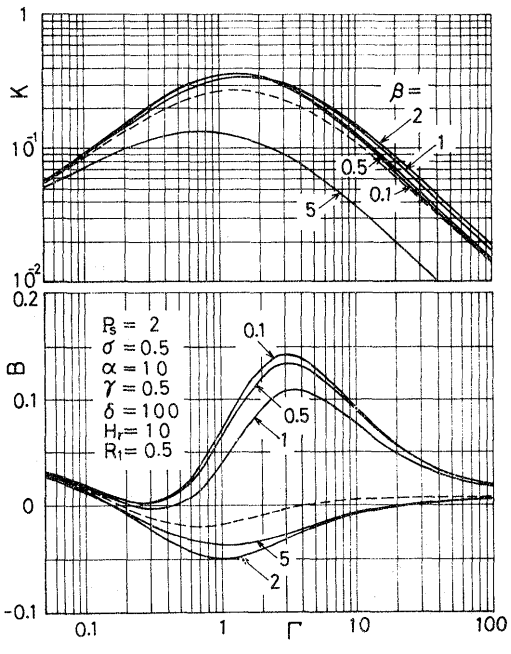

Fig.4 K, B for different β (Type A)

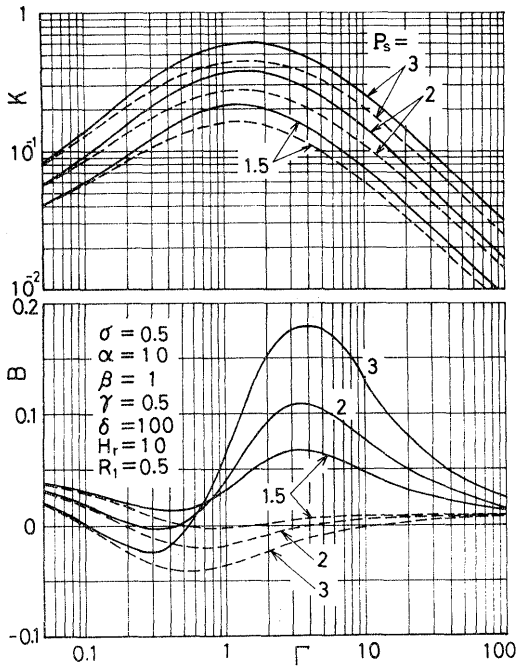

Fig.5 K, B for different P (Type A)

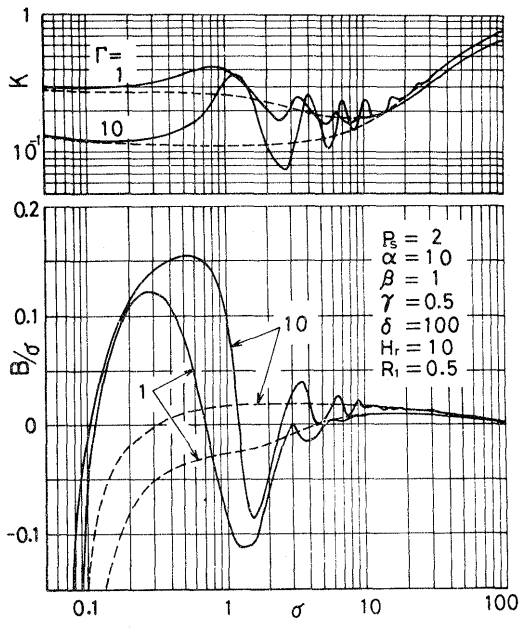

Fig.6 Variation of K, B with squeeze number (Type A)

in which the flow within the capillary restriction is treated quasisteadily are indicated with a broken line.

Figs.3 to 5 and 7 to 9 show the influence of α, β and P_s respectively on K and B. The influence is considerable when Γ takes the values for practical applications. In general, the inertia effect becomes remarkable as α increases in value. The influence on B becomes significant as P_s increases in value. In general, however, the influence of a change of P_s on K is not so remarkable.

Figs.6 and 10 show the influence of σ on K and B/σ. The influence on B is significant when σ decreases in value. In general, however, the influence of the inertia forces is not so remarkable when σ is large.

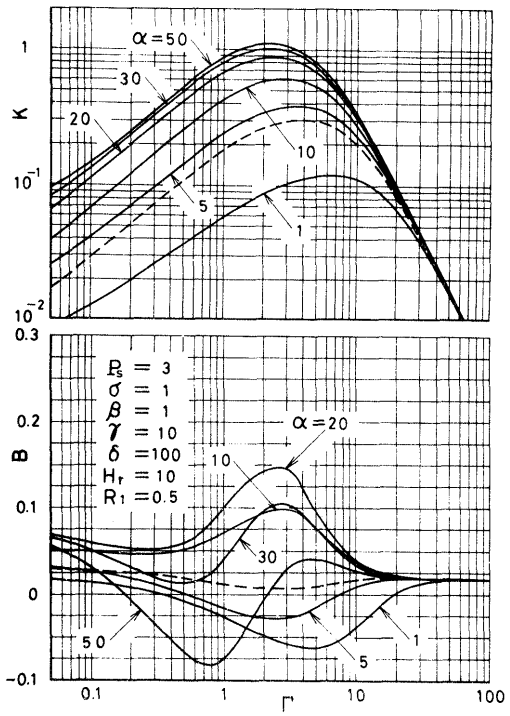

Fig.7 K, B for different α (Type B)

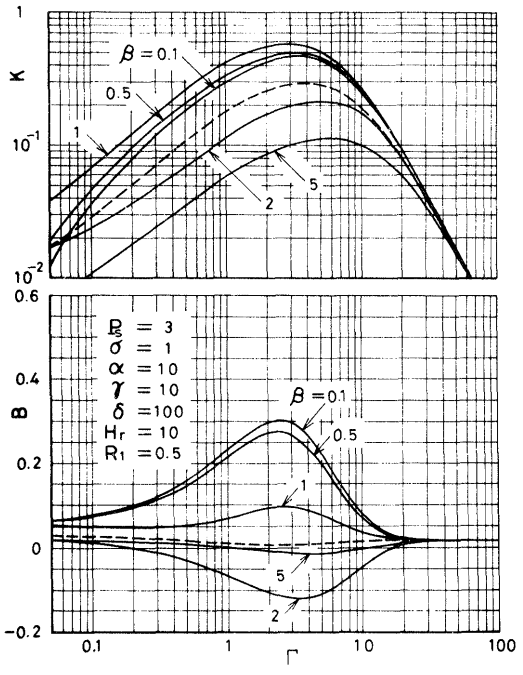

Fig.8 K, B for different β (Type B)

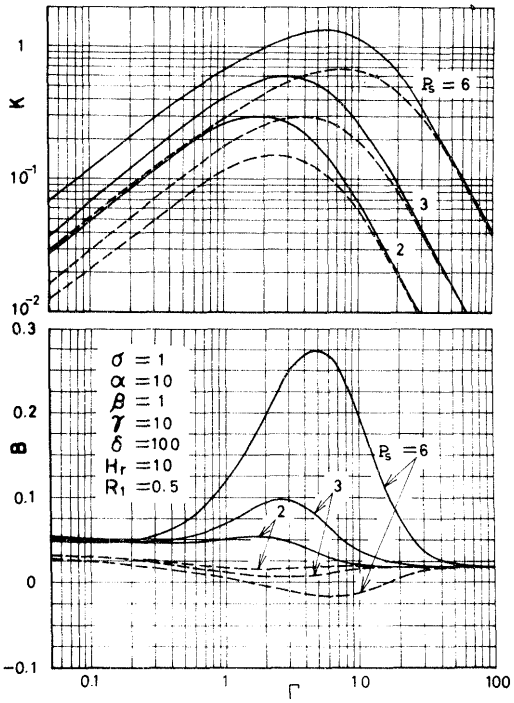

Fig.9 K, B for different P_s (Type B)

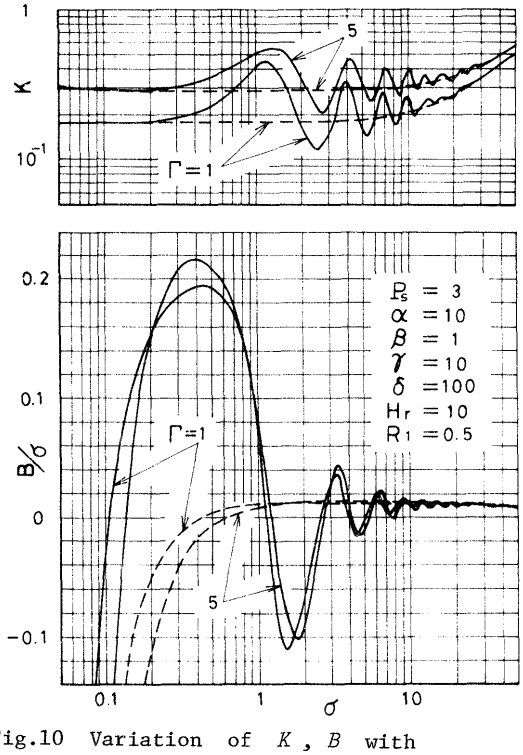

Fig.10 Variation of K, B with squeeze number (Type B)

5. Comparison with the experimental results

The experimental apparatus is schematically illustrated in Fig.11. A test bearing is fixed downward under the upper plate which is attached perpendicularly to the housing of the journal bearing. The upward thrust plate attached on the vertical shaft faces the test bearing. The shaft is supported by the test thrust bearing, the externally pressurized gas journal bearing and a back pressure of lower volume. The bearing clearance is set by adjusting the back pressure. The displacement of the thrust plate is measured by an electric capacitance micrometer.

Details of the test bearings are shown in Figs.12 and 13. Fig. 12 shows bearings of which the stabilizer is inserted into the gas supply line. Fig.13 shows a bearing of which the fluid capacity is connected to the bearing recess.

Experimental procedure is as follows: (1) Apply the supply pressure to the test bearing, (2) control the back pressure to get a specified value of the bearing clearance, (3) impose on the thrust plate an impulsive load and record the resulting vibration by a digital memory, and (4) analyze the frequency, f, and the logarithmic decrement, δ_0, by means of an oscilloscope.

K and B are analyzed experimentally from measured f and δ_0, by using the following relations

$$K=\frac{h_0}{\pi r_0^2 p_a} mf^2(4\pi^2+\delta_0^2) \tag{40}$$

$$B=\frac{h_0 2\pi f}{\pi r_0^2 p_a} 2mf\delta_0 \tag{41}$$

where m is mass of shaft { 1.50 kg (1.53×10^{-3} kgf s^2/cm) }.

In Figs.14 to 18, the theoretical estimations of K and B are compared with the experimental results. The volume of fluid capacity, V_c, is 100 cm^3. In these figures, the theoretical results in which the flow within the capillary restriction is treated quasisteadily are indicated with a broken line. In this experiment, the theoretical Reynolds number within the capillary restriction is 1800 or less. We use Perry's experimental equation[9] as discharge coefficient, c_D, of the supply orifice.

In Figs.14 to 16, it is seen that good agreement can be found between the estimations by the present theory and the experimental data and that the experimental data of K tend to deviate from the theoretical estimations.

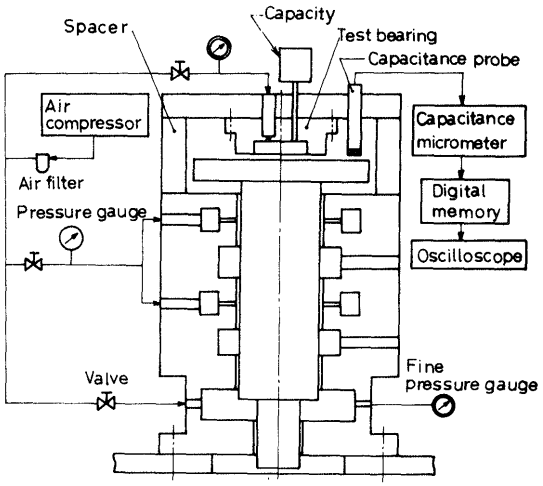

Fig.11 Schematic of experimental apparatus

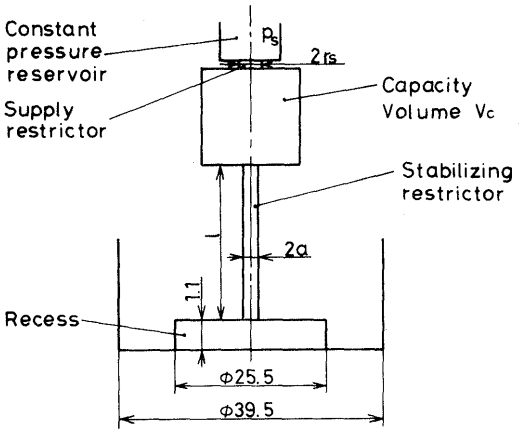

Bearing No.	a mm	l mm	n	r mm
1	0.27	100	10	0.25
2	0.50	200	3	0.35
3	0.95	250	1	0.25

Fig.12 Dimensions of test bearings (Type A)

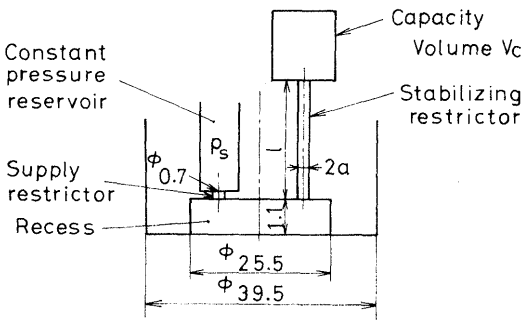

Bearing No.	a mm	l mm	n
4	0.50	300	1
5	0.95	1000	1

Fig.13 Dimensions of test bearings (Type B)

In Figs.17 and 18 good agreement can be found between the estimations by the present theory and the experimental data.

From these results, it may be concluded that the presented analysis yields good predictions for the dynamic characteristics of bearings in a wide range of designing conditions.

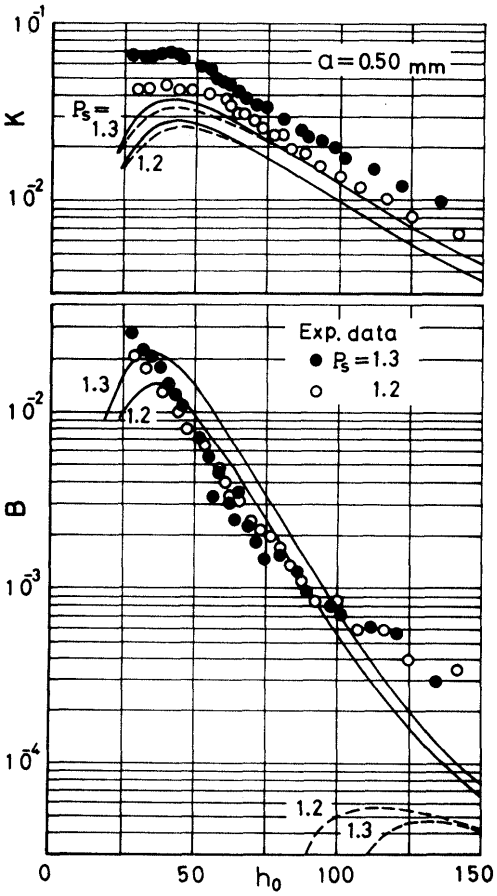

Fig.15 Comparison with experiment
(Bearing 2)

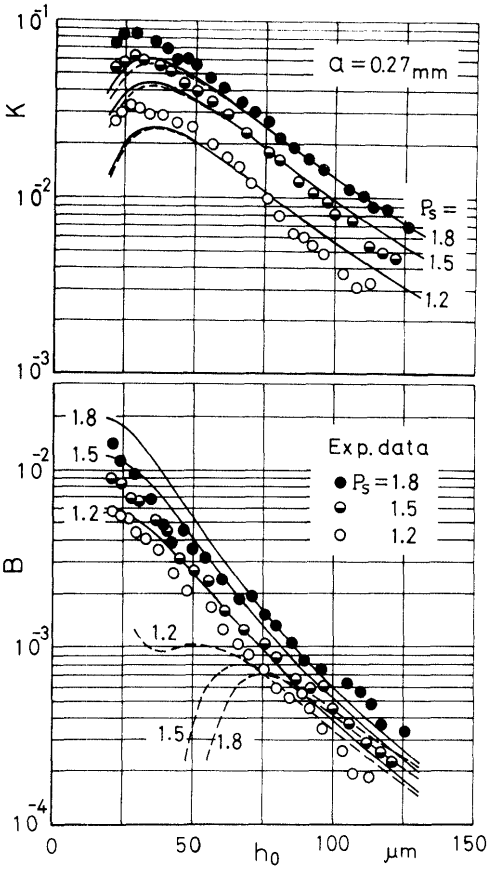

Fig.14 Comparison with experiment
(Bearing 1)

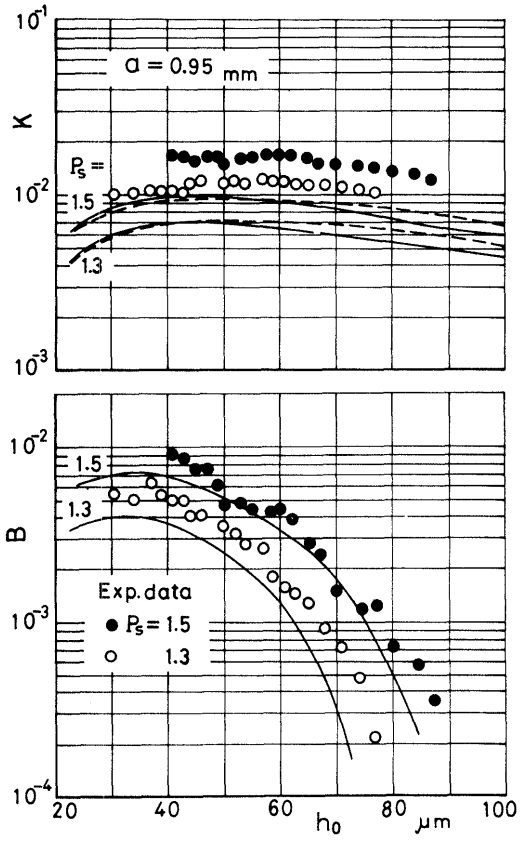

Fig.16 Comparison with experiment
(Bearing 3)

6. Conclusions

The influence of the gas inertia forces generated within the stabilizing restrictor on the dynamic characteristics of externally pressurized circular thrust gas bearings with a stabilizer was examined theoretically and experimentally. The stabilizer consists of a fluid capacity and a capillary restriction. The following conclusions have been obtained:

(1) The influence of the gas inertia forces can be determined by the inertia parameter, α, and the compressibility parameter, β. The influence is considerable when the feeding parameter, Γ, taks the values for practical applications.

(2) In general, the inertia effect becomes remarkable as the inertia parameter, α, increases in value.

(3) The influence on the damping coefficient becomes significant as the supply pressure, P_s, increases in value. In general, however, the influence of a change of the supply pressure, P_s, on the bearing stiffness is not so remarkable.

(4) The influence on the damping coefficient becomes significant when the squeeze number, σ, decreases in value. In general, however, the influence of the inertia forces is not so remarkable when the squeeze number, σ, is large.

Acknowledgement

The authors wish to express their gratitude to Prof. H. Yabe, Instructor U. Yamamoto, Instructor A. Mori, Instructor K. Ikeuchi, Kyoto University for their helpful advices and slso wish to acknowledge the consistent guidance and encouragement of Prof. T. Kazamaki, Toyama University.

References

(1) Mori, A., et al., Bull. JSME, Vol.22, No.173 (1979-11),p.1678.
(2) Mori, A., et al., Bull. JSME, Vol.23, No.178 (1980-4),p.582.
(3) Mori, A., et al., Bull. JSME, Vol.23, No.180 (1980-6),p.953.
(4) Haruyama, Y. et al., Bull. JSME, Vol. 25, No.200 (1982-2),p.284.
(5) Mori, H. and Mori, A., Trans. JSME (in Japanese), Vol.32, No.244 (1966-12),p.1877.
(6) Mori, H. and Mori, A., Trans. JSME (in Japanese), Vol.33, No.256 (1967-12),p.2065.
(7) Sato, K., Kyoto Univ., Doctor's Thesis (in Japanese), (1976),p.33.
(8) Ohmi, M. et al., Bull. JSME, Vol.19, No.129 (1976-3),p.298.
(9) Perry, J. A., Trans. ASME, Vol.71 (1949),p.757.

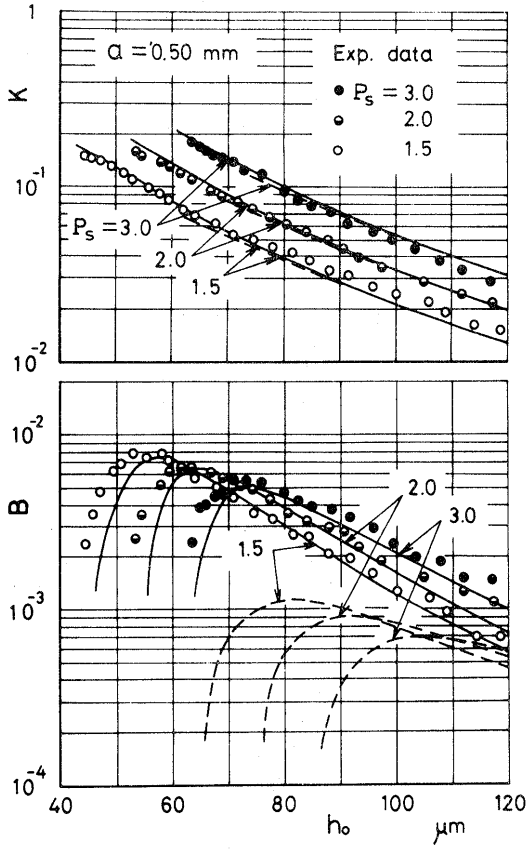

Fig.17 Comparison with experiment (Bearing 4)

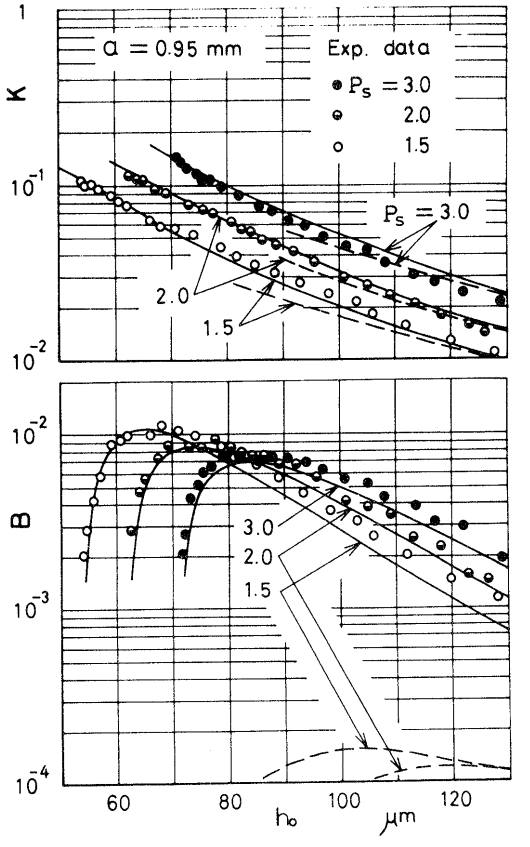

Fig.18 Comparison with experiment (Bearing 5)